

# Integrating photovoltaic and power converter characteristics for energy extraction study of solar PV systems

Shuhui Li\*, Timothy A. Haskew, Dawen Li, Fei Hu

Department of Electrical and Computer Engineering, University of Alabama, Tuscaloosa, AL 35487, USA

## ARTICLE INFO

### Article history:

Received 17 June 2010

Accepted 21 February 2011

Available online 25 May 2011

### Keywords:

Solar power

Photovoltaic cell

Power converter

Maximum energy extraction

Grid interface

Modeling and simulation

## ABSTRACT

Solar photovoltaic (PV) energy is becoming an increasingly important part of the world's renewable energy. A grid-connected solar PV system consists of solar cells for energy extraction from the sun and power converters for grid interface. In order for effective integration of the solar PV systems with the electric power grid, this paper presents solar PV energy extraction and conversion study by combining the two characteristics together to examine various factors that may affect the design of solar PV systems. The energy extraction characteristics of solar PV cells are examined by considering several practical issues such as series and parallel connections, change of temperatures and irradiance levels, shading of sunlight, and bypassing and blocking diodes. The electrical characteristics of power converters are studied by considering physical system constraints such as rated current and converter linear modulation limits. Then, the two characteristics are analyzed in a joint environment. An open-loop transient simulation using SimPowerSystem is developed to validate the effectiveness of the characteristic study and to further inspect the solar PV system behavior in a transient environment. Extensive simulation study is conducted to investigate performance of solar PV arrays under different conditions.

© 2011 Elsevier Ltd. All rights reserved.

## 1. Introduction

Investment in solar photovoltaic energy is rapidly increasing worldwide [1]. A grid-connected solar photovoltaic (PV) system consists of a PV generator that produces electricity from sunlight and power converters for energy extraction and grid interface control [2,3]. The smallest unit of a PV generator is a solar cell and a large PV generator is built by many solar cells that are connected together through certain series and parallel connections [4]. Unlike the traditional power generation, the operation of a grid-connected solar PV system depends on the coordination of the electrical system and PV cells under variable weather and system conditions. In order for an optimal design of the integrated system, it is important to investigate how the electrical characteristics of the power converter and the physics characteristics of the solar cells affect the design, energy extraction and grid integration of a solar PV system.

Traditionally, solar cell and power converter characteristics are usually inspected in separate environments at the PV generator and grid integration levels, respectively [2,4,5]. Different from previous studies [4–8], the main features of this paper are 1)

a study of power converter electrical characteristics using a d-q steady-state model, 2) an examination of extracted solar power characteristics under different weather and system conditions, 3) an integration of PV generator characteristics with power converter characteristics in a joint environment, and 4) a transient simulation assessment for comparison with the characteristic evaluations.

In the sections that follow, the paper first introduces the general configurations of a grid-connected solar PV system as well as the control strategies at the PV generator and power converter levels in Section 2. Section 3 presents a d-q steady-state model of the grid-connected power converter system and electrical characteristics of the power converter under different d-q control conditions. A solar cell model is presented in Section 4, which is used for energy extraction and grid integration study of the solar PV system by incorporating electrical characteristics of the power converter and extracted power characteristics of the PV generator together. Section 5 studies how temperature and insolation level variations would affect the power converter and PV generator. Section 6 investigates how the integrated PV generator and power converter are influenced when uneven sunlight is applied to solar cells. Section 7 presents integrated transient simulation evaluation of various parametric data of the PV system concurrently under different operating conditions. Finally, the paper concludes with the summary of main points.

\* Corresponding author.

E-mail address: [sli@eng.ua.edu](mailto:sli@eng.ua.edu) (S. Li).

## 2. Grid-connected solar PV systems

A grid-connected solar PV system consists of three parts: an array of solar cells, power electronic converters, and an integrated control system [9]. A solar cell is a semiconductor device that converts sunlight into direct-current electricity. Normally, solar cells are connected in series to form a module that gives a standard dc voltage. For an application, modules are connected into an array to produce sufficient current and voltage to meet a demand [4]. There are generally two ways to connect PV modules into an array. The first approach connects modules in series into strings and then in parallel into an array. The second approach first wires modules together in parallel and then those units are combined in series. For practical applications, PV system optimization methods are normally employed [10]. In practice, sizing the systems has been established based on system performance, component modeling, technical-economical considerations and system reliability [11]. Techniques of PV array optimization are especially useful for manufacturers who do not have detailed information about the future implementation of their products. The optimum configuration depends on the general radiative characteristics of the place, showing a clear dependence on latitude [12]. Several other PV array interconnection schemes known in practice are also reviewed in [13].

Ideally, both series-parallel and parallel-series connections are equivalent if all the cells and modules are identical and work at the same condition. But, if sunlight is applied unevenly to different PV cells as well as shading or other impacts, the second connection approach could cause many very bothersome problems [2]. The control system of a solar PV system contains two parts: one for maximum power point tracking (MPPT) and the other for grid interface control [14–17]. Both control functions are achieved through power electronic converters. There are three typical power converter configurations [18]: 1) a dual-stage converter configuration including a dc/dc boost converter performing the MPPT and a grid-connected dc/ac converter performing grid interface control, 2) a configuration with multi-string dc/dc converters and a grid-connected dc/ac converter, and 3) a single-stage dc/ac converter handling all the tasks such as MPPT and grid interface control. Fig. 1 shows a PV array with converter configuration 2.

For converter configurations 1 and 2, the voltage applied to each string is

$$V_s = (1 - D) \cdot V_{dc} \quad (1)$$

where  $V_{dc}$  is the dc-link voltage and  $D$  is the duty ratio of the boost dc/dc converter. For configuration 3, the dc-link voltage is applied

to the parallel strings directly. In general, the MPPT control is achieved by varying the dc voltage applied to the PV generator. Typical MPPT strategies include Perturb and Observe, Incremental Conductance, Voltage-Based MPPT and Current-Based MPPT.

In the Perturb and Observe approach, a slight dc voltage perturbation is introduced. If the output power of the PV generator increases, then the perturbation is continued in that direction. Otherwise, the perturbation is changed to the opposite direction. The process continues until the maximum power point (MPP) is reached [19,20].

In the Incremental Conductance approach, the perturbation voltage is calculated through the derivative of the output power over the PV generator dc voltage [21]. Hence, compared to the Perturb and Observe approach, the Incremental Conductance approach is faster and more stable to get to the MPP.

In the Voltage-Based MPPT approach, it is assumed that an MPP of a particular solar PV module lies at about 0.8 times the open circuit voltage of the module. Then, based on this relationship, a feed forward voltage control scheme can be implemented to bring the solar PV module voltage to the MPP [22]. However, the open circuit voltage and the MPP of the module vary with temperature and other factors so that the MPP for a practical PV application is hard to get by using this technique.

In the Current-Based MPPT approach, it is assumed that an MPP of a PV module lies at the point about 0.9 times the short circuit current of the module. Similar to the Voltage-Based approach, the short circuit current and the MPP of the module may be affected by insolation levels so that the MPP for a practical PV application is also hard to get by using this method [23].

## 3. Power control characteristics of grid-connected dc/ac converter

For all the three converter configurations, the dc/ac inverter operates on a similar principle, i.e., a control goal to assure the active power from the solar array being transferred to the ac grid and the reactive power of the ac system at a desired value while maintaining a high power quality in terms of harmonics and unbalance. Fig. 2 shows the schematic of the grid-connected dc/ac converter system, in which a dc-link capacitor is on the left, a three-phase voltage source representing the grid voltage at the Point of Common Coupling (PCC) is on the right, and a grid filter is in between.

In the  $d$ - $q$  reference frame, the voltage balance across the grid filter is [16,17]

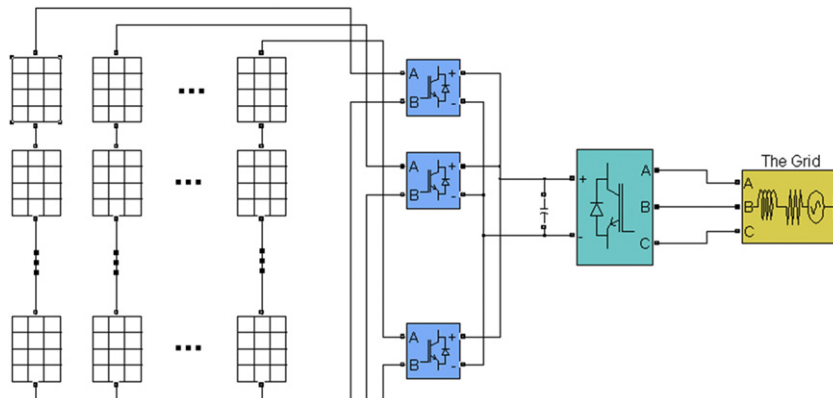


Fig. 1. Dual stage multi-string converter configuration of grid-connected photovoltaic systems.

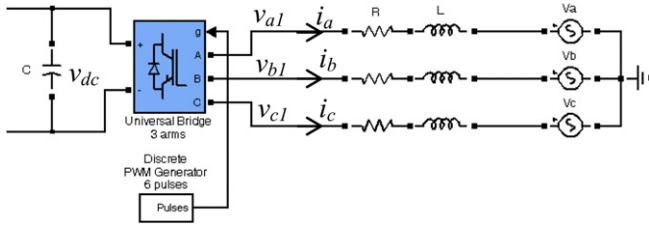


Fig. 2. Grid-connected dc/ac converter schematic.

$$\begin{bmatrix} v_{d1} \\ v_{q1} \end{bmatrix} = R \begin{bmatrix} i_d \\ i_q \end{bmatrix} + L \frac{d}{dt} \begin{bmatrix} i_d \\ i_q \end{bmatrix} + \omega_s L \begin{bmatrix} -i_q \\ i_d \end{bmatrix} + \begin{bmatrix} v_d \\ v_q \end{bmatrix} \quad (2)$$

where  $\omega_s$  is the angular frequency of the grid voltage, and  $L$  and  $R$  are the inductance and resistance of the grid filter. Using space vectors, Eq. (2) can be expressed by a complex Eq. (3) in which  $v_{dq}$ ,  $i_{dq}$ , and  $v_{dq1}$  are instantaneous space vectors of PCC voltage, line current, and converter injected voltage to the grid.

$$v_{dq1} = R \cdot i_{dq} + L \frac{d}{dt} i_{dq} + j\omega_s L \cdot i_{dq} + v_{dq} \quad (3)$$

Under the steady-state condition, (3) becomes:

$$V_{dq1} = R \cdot I_{dq} + j\omega_s L \cdot I_{dq} + V_{dq} \quad (4)$$

where  $V_{dq}$ ,  $I_{dq}$  and  $V_{dq1}$  stand for the steady-state space vectors of PCC voltage, grid current, and converter injected voltage to the grid.

The general approach used in the controller design of the grid-connected dc/ac converter is the PCC voltage oriented frame [16,17,24], i.e., the  $d$ -axis of the reference frame is aligned along the PCC voltage position. Hence, in terms of the steady-state condition,  $V_{dq} = V_d + j0$ . Assuming  $V_{dq1} = V_{d1} + jV_{q1}$  and neglecting the filter resistance, then, the steady-state current flowing between the PCC and the converter according to Eq. (4) is:

$$I_{dq} = \frac{V_{dq1} - V_{dq}}{jX_L} = \frac{V_{d1} - V_d}{jX_L} + \frac{V_{q1}}{X_L} \quad (5)$$

in which  $X_L$  stands for the grid filter reactance.

Supposing generator convention is applied, i.e., power flowing toward the grid as positive, then, the power transferred from the converter to the grid can be achieved from the basic complex power equation,  $P_g + jQ_g = V_{dq1} I_{dq}^* = V_d I_{dq}^*$ . By solving this power equation together with Eqs. (5), (6) is obtained,

$$P_g = \frac{V_d V_{q1}}{X_L}, \quad Q_g = \frac{V_d}{X_L} (V_{d1} - V_d) \quad (6)$$

According to Eq. (6), the active and reactive powers are controlled through  $q$  and  $d$  components  $V_{q1}$  and  $V_{d1}$  of the converter injected voltage to the grid, respectively. If the filter resistance is considered, the similar power control characteristics of the grid-connected converter still exist as shown by [25]. For any power control conditions, though, the converter must operate within the rated current and converter linear modulation limits as shown by Eq. (10) where  $I_{rated}$  is the rated phase rms current of the converter and  $V_{conv}$  is the phase rms voltage of the converter output voltage [26].

$$\sqrt{\frac{I_d^2 + I_q^2}{3}} \leq I_{rated}, \quad V_{conv} = \sqrt{\frac{V_{d1}^2 + V_{q1}^2}{3}} \leq \frac{V_{dc}}{2\sqrt{2}} \quad (10)$$

#### 4. Characteristics of solar PV arrays

Control of power converters in a solar PV system relies strongly on the PV generator characteristics. In most existing grid integration study of a solar PV array, a solar cell is modeled by a current source, representing the photogenerated current  $I_L$ , in parallel with a diode. For a practical solar cell, however, two additional effects must be considered, i.e., 1) current leaks proportional to the terminal voltage of a solar cell and 2) losses of semiconductor itself and of the metal contacts with the semiconductor [2,4,27]. The first is characterized by a parallel resistance  $R_p$  accounting for current leakage through the cell, around the edge of the device, and between contacts of different polarity (Fig. 3). The second is characterized by a series resistance  $R_s$ , which causes an extra voltage drop between the junction voltage and the terminal voltage of the solar cell for the same flow of current.

The relationship between the current  $I_c$  produced by a solar cell and the output voltage  $V_c$  of the cell is

$$I_c = I_L - I_0 \left( \frac{qV_d}{emkT} - 1 \right) - \frac{V_d}{R_p}, \quad V_c = V_d - I_c \cdot R_s \quad (11)$$

where the photocurrent  $I_L$  is proportional to the illumination intensity, the diode reverse saturation current  $I_0$  depends on temperature,  $m$  is diode ideality factor (1 for an ideal diode),  $q$  is the elementary charge,  $k$  is the Boltzmann's constant, and  $T$  is absolute temperature [2,4].

Important characteristics for a solar cell are output current  $I_c$  and output power  $P_c$  versus output voltage  $V_c$  characteristics. When considering both  $R_p$  and  $R_s$ , the characteristics of a solar cell are obtained by varying the voltage  $V_d$  applied to the diode and then computing  $I_c$  and  $V_c$  for each  $V_d$  value Eq. (11). The characteristics of a solar array are integration of all the solar cell characteristics. If assuming all the cells of a solar array are identical and function under the same conditions of illumination and temperature, then, the current  $I_a$  and terminal voltage  $V_a$  produced by the solar array are

$$I_a = N_p I_c \quad V_a = N_s N_c V_c \quad (12)$$

where  $N_c$  is the number of cells connected in series in a module,  $N_s$  is the number of modules connected in series in a string, and  $N_p$  is the number of strings connected in parallel (Fig. 1). For a given number of total modules in an array, the characteristics of a solar array depend on  $N_p$  and  $N_s$ . In general, for modules in series, the  $I$ - $V$  curves are added along the voltage axis; for modules in parallel, the  $I$ - $V$  curves are added along the current axis. Regarding the  $P$ - $V$  characteristics, the maximum extracted power is almost not affected by  $N_p$  and  $N_s$ . However, the  $P$ - $V$  characteristics extend or shrink along the voltage axis depending on the number of modules in a string. It is also found from the simulation study that if all the cells operate at the same condition, the MPP voltage  $V_{amax}$  of the solar array can be estimated from the MPP voltage  $V_{cmax}$  of a solar cell by

$$V_{amax} = N_s N_c V_{cmax} \quad (13)$$

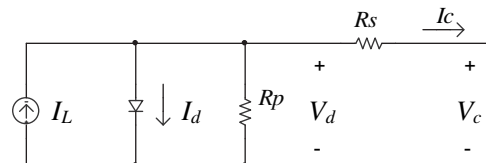


Fig. 3. Solar cell equivalent circuit model.

Although the maximum extracted power does not change with  $N_p$  and  $N_s$ , how to select the values of  $N_p$  and  $N_s$  affects the power converters for MPPT and grid interface control. Assuming the maximum extracted power from a solar array is  $P_{amax}$  and the grid reactive power should be zero, then, according to Eq. (6) the  $q$  and  $d$  components of the converter output voltage should be:

$$V_{q1} = \frac{X_L P_{amax}}{V_d}, V_{d1} = V_d \quad (14)$$

Therefore, to meet the converter linear modulation constraint, the dc capacitor voltage according to Eq. (10) should satisfy the following condition:

$$V_{dc} \geq V_{dc_{min}} = 2\sqrt{\frac{2}{3}\left(V_d^2 + \left(\frac{X_L P_{amax}}{V_d}\right)^2\right)} \quad (15)$$

Hence, for converter configurations 1 and 2, the dc-link voltage  $V_{dc}$  must be maintained, through the control of the grid-connected dc/ac converter, at a reference value  $V_{dc_{ref}}$  that is larger than  $V_{dc_{min}}$ . If a  $V_{dc_{ref}}$  is selected, then, the MPPT control by the dc/dc converters requires that the number of the series modules in a string according to Eqs. (13) and (1) should satisfy

$$N_s \leq \frac{V_{dc_{ref}}}{N_c V_{cmax}} \quad (16)$$

Nevertheless, this situation is different for converter configuration 3 since the dc/ac converter is used for both the MPPT and grid interface control. From the converter linear modulation standpoint, control of the grid-connected dc/ac converter must maintain a dc-link voltage that satisfies Eq. (15). Since this dc voltage is also used for MPPT control of the solar PV array, the number of series modules in a string must be large enough so that  $V_{amax} > V_{dc_{min}}$  from the MPPT control requirement perspective. Therefore, different from converter configurations 1 and 2,  $N_s$  must meet the following condition for converter configuration 3 according to Eqs. (13) and (15).

$$N_s \geq \frac{2}{N_c V_{cmax}} \sqrt{\frac{2}{3}\left(V_d^2 + \left(\frac{X_L P_{cmax}}{V_d}\right)^2\right)}. \quad (17)$$

## 5. Temperature and insolation impact to converter and PV array integration

### 5.1. Effect of temperature

Temperature affects the characteristic Eq. (11) of a solar cell primarily in the following two ways: directly via  $T$  in the exponential

term of Eq. (11) and indirectly via its effect on the reverse-bias saturation current  $I_0$ . The impact of temperature to photocurrent  $I_L$  is small and can be ignored [2]. The dependence of the reverse-bias saturation current  $I_0$  on temperature for a silicon solar cell is

$$I_0(T) = K \cdot T^3 \cdot e^{-\frac{E_{GO}}{kT}} \quad (18)$$

where  $K$  and  $E_{GO}$  (the bandgap at 0 K) are both approximately constant with respect to temperature [2,4]. The overall effect of temperature on solar PV array characteristics can be studied by considering Eq. (18) in Eqs. (11) and (12). In general, as the temperature increases, the MPP voltage reduces and the MPP power drops significantly, indicating that photovoltaic cells perform better on cold days than hot ones. Therefore, the temperature affects the integration of PV generator with power converters. Fig. 4 shows  $V_{amax}$  vs.  $N_s$  characteristics as well as  $V_{dc_{min}}$  calculated using Eq. (15) for four different temperatures. As it can be seen from the figure, under the same  $N_s$  value, the higher the temperature, the smaller the MPP voltage. But,  $V_{dc_{min}}$  changes very little. Thus, for converter configurations 1 and 2, if the MPP voltage is above the dc-link voltage due to a low temperature, the MPPT control effectiveness will be affected; for converter configuration 3, if MPP voltage is below  $V_{dc_{min}}$  due to a high temperature, the dc/ac converter may not be able to maintain the effectiveness of both MPPT and grid interface controls. Those factors must be considered in designing a solar PV system. Otherwise, the efficiency and stability of the overall system could be affected in a feedback control environment.

### 5.2. Effect of illumination intensity

Over a wide operating range, the photocurrent of a solar cell is directly proportional to the intensity of irradiance levels. If the photocurrent at the level of irradiance defined as unity is  $I_{L1}$ , then, the photocurrent at a level of irradiance  $X$  can be approximated by  $I_L = X \cdot I_{L1}$  [2]. Although this approximation behaves worse with increasing concentration, the photocurrent usually increases with the increase of the level of irradiance. Therefore, conclusions obtained based on this approximation should still be applicable to common cases. For different irradiance levels, the  $I-V$  and  $P-V$  characteristics of a solar array can be investigated by considering the property of  $I_L = X \cdot I_{L1}$  in Eqs. (11) and (12). In general, as the irradiance level decreases, the maximum power drops greatly but the MPP voltage remains almost unchanged. Similar to Fig. 4, the required minimum dc-link voltage  $V_{dc_{min}}$  calculated using Eq. (15) does not change much. Hence, unlike results obtained in Section 5.1, the change of irradiance levels has very little impact to MPPT and grid interface control of a solar PV system.

The study presented above shows that as the temperature or illumination intensity varies, the MPP voltage may change and the maximum extracted solar power may change [28] but the required minimum dc-link voltage  $V_{dc_{min}}$  does not change much.

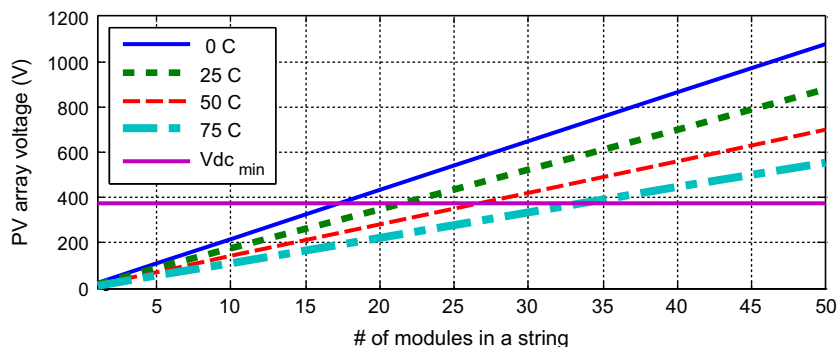


Fig. 4.  $V_{dc_{min}}$  and MPP voltage vs.  $N_s$  characteristics for PV array varying cell temperatures ( $N_p = 10$ ,  $N_s = 20$ ,  $N_c = 36$ ).

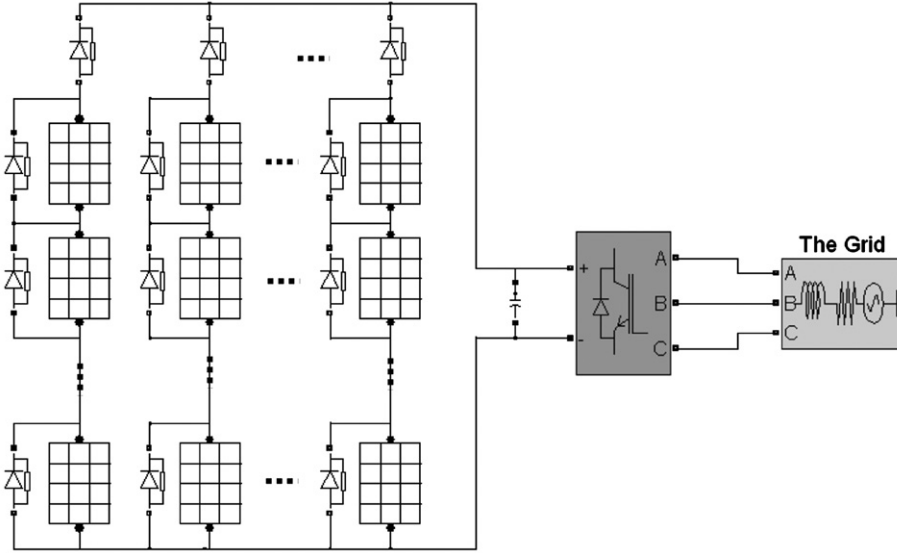


Fig. 5. Bypass and blocking diodes in a solar PV generator.

Traditionally, control goals of the grid-connected dc/ac converter include (i) assuring active power to be transferred from the solar PV array to the grid, and (ii) compensating the reactive power absorbed from the grid by the converter completely. However, under the constraint of Eq. (10), it may be impossible to find  $V_{d1}$  and  $V_{q1}$  that satisfy both control requirements at the same time, particularly as temperature changes (Fig. 4). Hence, due to the converter rated power and linear modulation constraints, it is appropriate to develop a new control strategy, in which the primary control goal should be to maintain active power control effectiveness, i.e., keeping the maximum power extracted by the PV array ( $P_{amax}$ ) equal to the power transferred to the grid through the converter ( $P_{grid}$ ) when neglecting the converter losses, and the secondary control goal should be to keep the resultant reactive power absorbed from the grid by the PV system  $Q_{grid}$  as close as possible to the reactive power reference  $Q_{grid}^*$ . This results in a nonlinear programming or an optimal control strategy as illustrated below.

$$\text{Minimize : } |Q_{grid} - Q_{grid}^*|$$

$$\text{Subject to : } P_{grid} = P_{amax}, \sqrt{\frac{I_d^2 + I_q^2}{3}} \leq I_{rated}$$

$$V_{conv} = \sqrt{\frac{V_{d1}^2 + V_{q1}^2}{3}} \leq \frac{V_{dc}}{2\sqrt{2}}$$

### 6. Shading impacts to PV array and power converter integration

The analysis in the above sections is based on the assumption that all the cells and modules making up the PV generator are identical and work under the same condition. But in reality, the characteristics of the cells and modules are subject to some variations. This may happen when uneven sunlight is applied to a solar PV array, unclean PV cells, variation of the cell parameters to be expected from manufacturing process, or other conditions [2,4]. When a PV cell is shaded, for example, the photocurrent in a module or a string has to pass through the parallel resistance  $R_p$  of the cell as shown in Fig. 3. This means that the shaded cells, instead of adding to the output voltage and power, actually reduce it. Therefore, even a single shaded cell in a long string of cells can easily cut output power by more than half and create potential damaging hot spots in the shaded cell [2,4]. Thus, external bypass diodes are normally utilized to mitigate the impacts of shading on  $P-V$  curves as shown by Fig. 5. In addition, blocking diodes are also used at the top of each string to prevent a shading or malfunctioning string from withdrawing current from the rest strings that are wired together in parallel.

The shading influence to the  $P-V$  characteristics of a solar array depends on the distribution of the shaded cells within the PV array. Assuming the bypass diodes are ideal, then, the diode of a module turns on when the photogenerated voltage of the module is less than the voltage drop over  $R_p$  of the shaded cells in the module. Hence, output power from a series string should be computed by

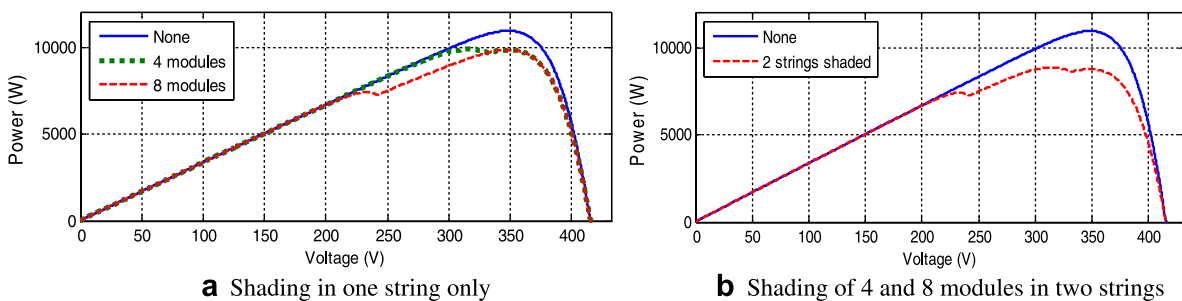


Fig. 6. Solar array characteristics under shading condition ( $T = 25\text{ }^\circ\text{C}$ ,  $N_p = 10$ ,  $N_s = 20$ ,  $N_c = 36$ ).

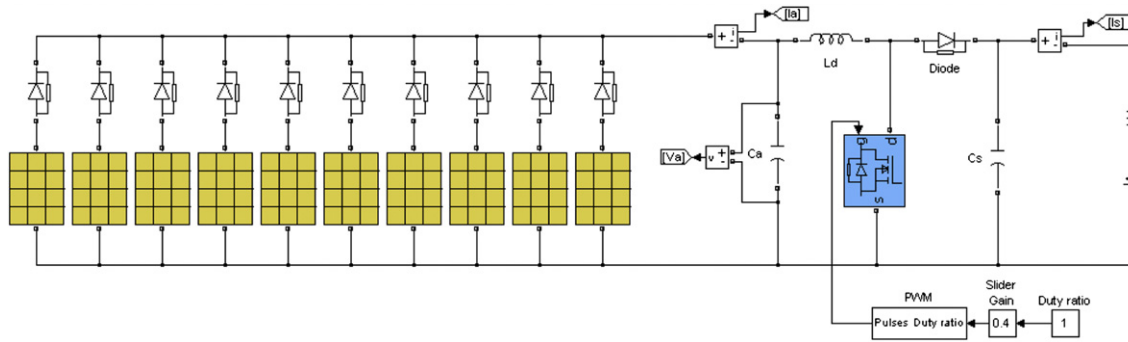


Fig. 7. Solar PV generator under the control of a dc/dc power converter using SimPowerSystems.

considering whether the voltage drops of the shaded cells within a module cause the bypass diode turning on or off. If there are  $n$  cells that are 100% shaded within one module while the rest cells within the module is in full sun, the current, voltage and power equations of one string containing the shaded module are:

$$\begin{cases} I_s = I_c = I_L - I_0 \left( \frac{qV_d}{mkT} - 1 \right) - \frac{V_d}{R_p} \\ V_s = (N_s N_c - n) [V_d - I_c \cdot R_s] - n \cdot I_c R_p, \text{ bypass diode is off} \\ V_s = (N_s - 1) N_c [V_d - I_c \cdot R_s], \text{ bypass diode is on} \\ P_s = I_s V_s \end{cases} \quad (19)$$

where  $I_s$ ,  $V_s$ , and  $P_s$  are output current, voltage and power of the string. It can be calculated from Eq. (19) that with the bypass diodes, the output power of a single PV string can be improved considerably if all the shaded cells only exist in one module. But, if there are more modules containing shaded cells, the  $I-V$  and  $P-V$  characteristics are more complicated. In general, the  $I-V$  or  $P-V$  characteristics of a string when considering shading impact depend on how many modules are shaded, how many cells within a module are shaded, and how much each cell is shaded. For an array of PV modules, the  $I-V$  and  $P-V$  characteristics of the array also depend on how many strings contain shaded cells.

For a solar PV array with  $N_s = 20$  and  $N_p = 10$ , Fig. 6a shows the  $P-V$  characteristics of the array under the conditions that 1) none of the cells in the array are shaded, 2) only four modules in one string contain 100% shaded cells and the rest cells of the PV array are in full sun, and 3) only eight modules in one string have 100% shaded cells and the rest cells of the PV array are in full sun. Fig. 6b shows the  $P-V$  characteristics of the solar array under the condition that four modules in one string contain 100% shaded cells, eight modules in another string contain 100% shaded cells, and the rest modules of the PV array are in full sun. As shown by Fig. 6, under a shaded condition, the  $P-V$  characteristics may have multiple peaks depending on the shading distribution over the cells in the PV array. This result implies that using conventional MPPT control mechanisms (Section 2), it is possible to get into a local MPP under a shading condition for a PV system using converter configurations 1 and 3, which would greatly reduce the efficiency of the solar PV array when a local MPP is reached. In order to get to the global MPP, new control strategies must be developed if converter configurations 1 and 3 are adopted. For converter configuration 2, however, MPPT control is obtained separately for each individual string by controlling the dc/dc converter of each string so that the maximum output power of the system is the summation of MPP powers of all the strings.

It is necessary to point out that the global MPP power obtained for converter configurations 1 and 3 is different from the summation of MPP powers obtained for converter configuration 2.

In general, the ratio of global MPP power of a PV array over the summation of MPP powers of all the PV strings varies depending on the shading distribution. For a PV array having only two strings of PV modules in parallel, in which PV cells in one string operate in full sun while the PV cells in the other string may be shaded, it was found that the lowest ratio occurs around a point that half of the modules contain 100% shaded cells in one string while all the PV cells in the other string operate in full sun.

### 7. Integrative study of solar PV system

The solar PV system is further investigated and verified through an integrative transient simulation method. The transient simulation of the solar PV system is developed by using MatLab SimPowerSystems. In the transient environment, characteristics of the solar

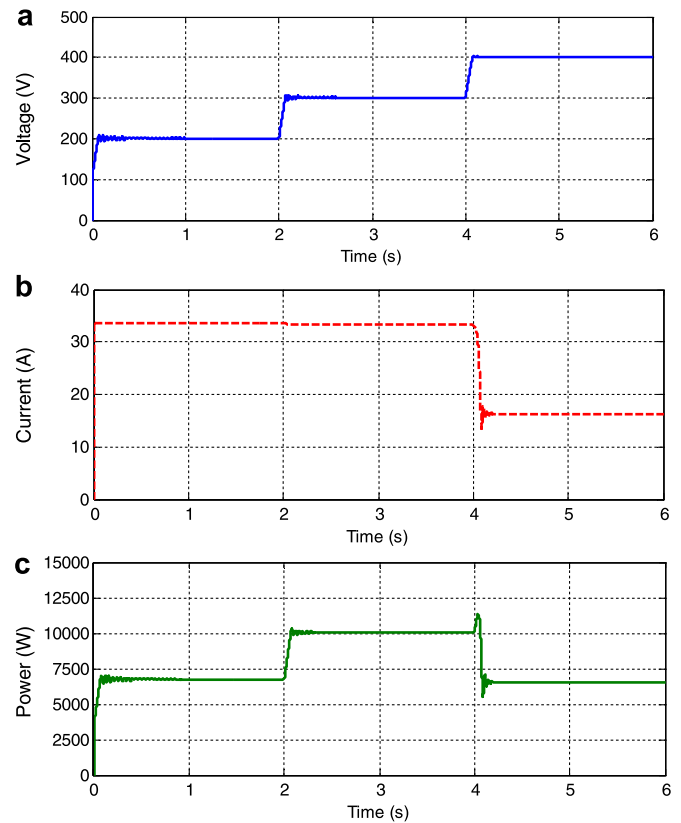


Fig. 8. Transient simulation results of a PV array when all cells operate at the same condition: a) Voltage applied to the PV array, b) Photogenerated current, c) PV array output power.

PV system are investigated under more realistic conditions, which include 1) actual circuit connection of the solar PV array, 2) high switching frequency power converters, 3) blocking and bypassing diodes, and 4) losses of the power converters and the system. Fig. 7 shows the transient simulation schematics of the solar PV system in an open-loop control condition for converter configurations 1 and 2. The dc voltage source represents the dc-link voltage between the dc/dc converter and the dc/ac inverter. The dc/dc converter is a boost converter, i.e., power flows from the PV array to the dc voltage source. Each string of PV modules is represented by a subsystem containing all the PV modules in series with a blocking diode on the top. The number of series and parallel PV modules are 20 and 10, respectively. Major measurements include current and voltage of each PV module, current and voltage of the PV array, and the photogenerated power of the PV array. For the power measurement, generator sign convention is used, i.e., power generated by the PV array and transferred to the dc source is positive.

Fig. 8 demonstrates transient results when all the PV cells are in the sun and operate at the same condition. The dc source voltage is 500 V. Before  $t = 2$  s, the duty ratio  $D$  of the dc/dc converter is 0.6. After the system is stable, the dc voltage applied to the PV array is 200.7 V (Fig. 8a) which is very close to the theoretical calculation of  $(1-D) \cdot V_{dc}$  for the dc/dc converter. The photogenerated current and power of the PV array are around 33.6 A and 6.7 kW, respectively, which are consistent with the steady-state results that can be obtained by solving (19). At  $t = 4$  s, the duty ratio of the dc/dc converter changes to 0.4 causing the terminal voltage of the boost dc/dc converter rising up. However, the output current of the PV array does not change much (Fig. 8b), reflecting that the PV cells still operate near the constant current region. At  $t = 6$  s, the duty ratio of the dc/dc converter changes to 0.2 and the voltage applied to the PV array increases to 400. At this voltage level, the output current of the PV cells decrease due to the equivalent diode effect and the output power of the PV array drops too (Fig. 8c). All the transient results after the PV system is stable for each control condition change are consistent with the steady-state results that can be calculated from Eq. (19), demonstrating the effectiveness of both transient and steady-state computations.

## 8. Conclusions

This paper presents an energy extraction and grid interface control study of a solar PV system by combining the energy extraction characteristics of the PV generator and the electrical characteristics of the power converters jointly in one environment for an integrative investigation.

Through the integrated study, it is found that the operation of a solar PV system is determined by the PV generator, the dc-link voltage and the power converters. If an ac/dc/dc converter configuration is used between the grid and the PV array, the dc-link voltage must be designed to be larger than the highest of the following two voltage values: 1) the maximum MPP voltage of the PV array for all the possible temperatures and irradiance levels, and 2) the dc-link voltage that can meet reactive power compensation requirement under the highest possible power transferred from the PV array to the grid. If only an ac/dc converter is used between the grid and the PV array, the series number of solar PV array must be selected in such a way that the minimum MPP voltage of the PV array for all the possible temperatures and irradiance levels must be large enough so that the ac/dc converter can meet reactive power compensation need under the highest possible power transferred from the PV array to the grid. Otherwise, maximum power extraction of the PV array and/or the proper operation of the ac/dc converter may be affected. To assure stable and reliable operation of a solar PV system while maximizing the power transferred from the PV generator to the grid for all conditions, it is

beneficial to develop an optimal control mechanism for the grid-connected dc/ac converter.

Under uneven shading situations, the  $P$ – $V$  characteristics of a PV array may exhibit multiple peaks because the peak power of each PV string does not appear at the same external voltage applied to the PV array. Thus, if using an ac/dc converter or an ac/dc/dc converter between the grid and PV array, the MPPT control strategy must be designed to be able to locate the highest peak power production of the PV array. But, if using an ac/dc converter plus multiple dc/dc converters, each dc/dc converter connected to a string of PV modules is able to find the peak power production of that PV string, and the total power production of all the strings is the summation of the peak powers of all strings, making the multiple dc/dc converter structure has the highest efficiency compared to the other two converter configurations.

## Acknowledgment

This work was supported in part by the U.S. National Science Foundation under Grant 1059265.

## References

- [1] Global trends in sustainable energy investment 2007. United Nations Environment Programme/New Energy Finance Ltd; 2007.
- [2] Lorenzo E, Araujo G, Cuevas A, Egido M, Miñano J, Zilles R. Solar electricity: engineering of photovoltaic systems. Progensa; 1994.
- [3] Carrasco JM, Franquelo LG, Bialasiewicz JT, Galván E, Guisado RCP, Á M, et al. Power-electronic systems for the grid integration of renewable energy sources: a Survey. IEEE Trans Ind Electronics August, 2006;53(No. 4).
- [4] Nelson J. The physics of solar cells. London: Imperial College press; 2003.
- [5] Figueres E, Garcera G, Sandia J, Gonzalez-Espin F, Rubio JC. Sensitivity study of the dynamics of three-phase photovoltaic inverters with an LCL grid filter. IEEE Trans Ind Electronics March 2009;56(No. 3):706–17.
- [6] Liu F, Duan S, Liu F, Liu B, Kang Y. A variable step size INC MPPT method for PV systems. IEEE Trans Ind Electronics Jul. 2008;55(No. 7):2622–8.
- [7] Sera D, Teodorescu R, Hantschel J, Knoll M. Optimized maximum power point tracker for fast-changing environmental conditions. IEEE Trans Ind Electronics Jul. 2008;55(No. 7):2629–37.
- [8] Chen Y, Wu H, Chen Y. DC Bus regulation strategy for grid-connected PV power generation system. In: Proceedings of IEEE International Conference on Sustainable Energy Technologies. Singapore: ICSET 2008; Nov. 24–27, 2008.
- [9] Masters GM. Renewable and efficient electric power systems. Wiley-IEEE Press, ISBN 978-0-471-28060-6; 2004.
- [10] Kalaitzakis K. Optimal PV system dimensioning with obstructed solar radiation. Renew Energy 1996;7(1):51–6.
- [11] Bhatt MS, Kumar RS. Performance analysis of solar photovoltaic power plants-experimental results. Int J Renew Energy Eng 2000;2(2):184–92.
- [12] Badescu V. Simple optimization procedure for silicon-based solar cell interconnection in a series-parallel PV module. Energy Conversion Manage 2006; 47:1146–58.
- [13] Gautam NK, Kaushika ND. Reliability evaluation of solar photovoltaic arrays. Solar Energy 2002;72(2):129–41.
- [14] Tse KK, Ho MT, Henry, Chung SH, Hui SY. A novel maximum power point tracker for PV panels using switching frequency modulation. IEEE Trans Power Electronics 2002;17(6):980–9.
- [15] Veerachary M, Senjyu T, Uezato K. Maximum power point tracking control of IDB converter supplied PV system. IEE Proc Electr Power Appl 2001;148(6):494–502.
- [16] Moreno JC, Espí Huerta JM, Gil RG, González SA. A robust predictive current control for three-phase grid-connected inverters. IEEE Trans Ind Electronics October 2009;56(No. 6):1993–2004.
- [17] Rodríguez J, Pontt J, Silva CA, Correa P, Lezana P, Cortes P, Ammann U. Predictive current control of a voltage source inverter. IEEE Trans Ind Electronics Feb. 2007;54(No. 1):495–503.
- [18] Casaro MM, Martins DC. Behavior matching technique applied to a three-phase grid-connected PV system. In: Proceedings of IEEE International Conference on Sustainable Energy Technologies. Singapore: ICSET 2008; Nov. 24–27, 2008.
- [19] Hua C, Lin J, Shen C. Implementation of a DSP controlled photovoltaic system with peak power tracking. IEEE Trans Ind Electronics Feb 1998;45(No. 1):99–107.
- [20] Femia N, Petrone G, Spagnuolo G, Vitelli M. Optimization of perturb and observe maximum power point tracking method. IEEE Trans Power Electronics July 2005;20(No. 4):963–73.
- [21] Hussein KH, Muta I, Hoshino T, Osakada M. Maximum photovoltaic power tracking: an algorithm for rapidly changing atmospheric conditions. IEE Proceedings-Generation, Transm Distribution Jan 1995;142(No. 1):59–64.
- [22] Veerachary M, Senjyu T, Uezato K. Voltage-based maximum power point tracking control of PV system. IEEE Trans Aerospace Electronic Syst Jan. 2002; 38(No. 1):262–70.

- [23] Tafticht T, Agbossou K, Doumbia ML, Chériti A. An improved maximum power point tracking method for photovoltaic systems. *Renewable Energy* July 2008; 33(No. 7):1508–16.
- [24] Mullane A, Lightbody G, Yacamini R. Wind-turbine fault ride-through enhancement. *IEEE Trans Power Syst* Nov. 2005;20(No. 4).
- [25] Li S, Haskew TA. Transient and steady-state simulation of Decoupled d-q vector control in PWM converter of variable speed wind turbines. In: *Proceedings of 33rd Annual Conference of IEEE Industrial electronics*. Taipei, Taiwan: IECON 2007; Nov. 5–8, 2007.
- [26] Li S, Haskew TA, Jackson J. Power generation characteristic study of integrated DFIG and its frequency converter. *Renewable Energy (Elsevier)* Jan. 2010; 35(No. 1):42–51.
- [27] Gow JA, Manning CD. Development of photovoltaic array model for use in power-electronics simulation studies. *IEE Pro.-Electr Power Appl* Mar. 1999; 146(No. 2):193–200.
- [28] Mutoh N, Ohno M, Inoue T. A method for MPPT control while searching for parameters corresponding to weather conditions for PV generation systems. *IEEE Trans Ind Electron* Jun. 2008;53(No. 4):1055–65.